Send Orders for Reprints to reprints@benthamscience.ae

Open Access

A Study on the Static Stability of Scissor Lift

Wei Zhang[*,1,2,3], Chen Zhang[2], Jiangbo Zhao[3] and Chunzhi Du[1]

[1]*Airport College, Civil Aviation University of China, 100 Road Xunhai, Tianjin, P.R. China*

[2]*Sino-European Institute of Aviation Engineering, 100 Road Xunhai, Tianjin, P.R. China*

[3]*Aviation Ground Special Equipment Research 100 Road Xunhai, Tianjin, P.R. China*

Abstract: This paper studies the static stability of six kinds of scissor lifts with one input force of hydraulic actuator, and the input is on the lines of the nodes of the scissor lifts. Firstly the static stability of single scissor arm is studied by using energy method and modeling method in the software Nastran. The stability results of two methods are compared. Then the scissor lift models with hydraulic actuators are made to analyze the static stability. The static stability of six kinds of scissor lifts are compared. The results of the overall model are closer to the actual situation. By analyzing single arm models it is easier to compare theoretical solutions and modeling solutions, thus the study of stability of single scissor arm is meaningful.

Keywords: Scissor lift, static stability, energy method, finite element method.

1. INTRODUCTION OF SCISSOR LIFTS WITH DIFFERENT INPUT VECTORS

Scissor lifting mechanism is a typical lift machine [1-6] which has many advantages such as stable structure [4], reliable operation [1], high efficiency [2, 3, 5] and low failure rate [2, 6], etc. As a key component of platforms, the stability of scissors lifting mechanism determines the safety of the platform equipment [1, 6]. The instablility of scissor lift will make agency staff wounded or even death. In this paper, models of single scissor arm are made by using Finite Element software. The Critical load is calculated by buckling analysis. The theoretical results of critical loads are calculated by using energy method. The two results of modeling and energy method are compared. The FEM models of the total scissor lifts mechanism are made and the stability of scissor lifts with different input vectors are compared.

For a scissor lift with one input force of hydraulic actuator, and the input is on the lines of the nodes of the scissor lifts, there are 6 different kinds of scissor lifts in total, as shown in Fig. (**1**).

2. RELATED DATA OF MODELS

The main parts of scissor lifts are two scissor arms, a hydraulic actuator and a platform. The models are simplified as two dimension models with a hypothesis that the load W is fixed in the middle of the platform. The actuator force is P, the length of two scissor arms are 2 *L* with their number shown in Fig. (**2**).

The first kind of scissor lift is shown with the angle between ground and the scissor arm, the blue line represents the hydraulic actuator. All the references of the scissor lift are shown in Fig. (**2**).

The material of the scissor arm is aluminum alloy, with Young's modulus 70 GPa, Poisson ratio 0.3 and density $2.5\times10^{-6}\,kg/mm^3$. The material of the hydraulic actuator is steel with Young's modulus 200 GPa, Poisson ratio 0.3, and density is $7.8\times10^{-6}\,kg/mm^3$.

Based on the equation of input hydraulic force and the load, we can get

$$P=\frac{2Wl}{N\sin\theta+M\cos\theta\tan\alpha} \tag{1}$$

The references *M* and *N* in the six cases are shown in Table **1**.

For all the rest of the research the data of all references are given:*l*=600mm, *W*=2000N, the valuevaries from 15 degree to 45 degree. All the other data of references are shown in Table **2**.

The cross section of the scissor arm is shown in Fig. (**3**), with the data *B*=30 mm, *H*=50 mm, *b*=24 mm, *h*=44 mm.

The area of the cross section, and the inertial moment.

$$A=HB-hb=444\,mm^2$$

$$I=\frac{BH^3-bh^3}{12}=142000\text{mm}^4$$

3. STATIC ANALYSIS OF RIGID BODY

In order to analyze the stability of scissor arms, the internal forces of the nodes must be calculated. Each of the five nodes are given a number. In the coordinate system the

1874-155X/15 2015 Bentham Open

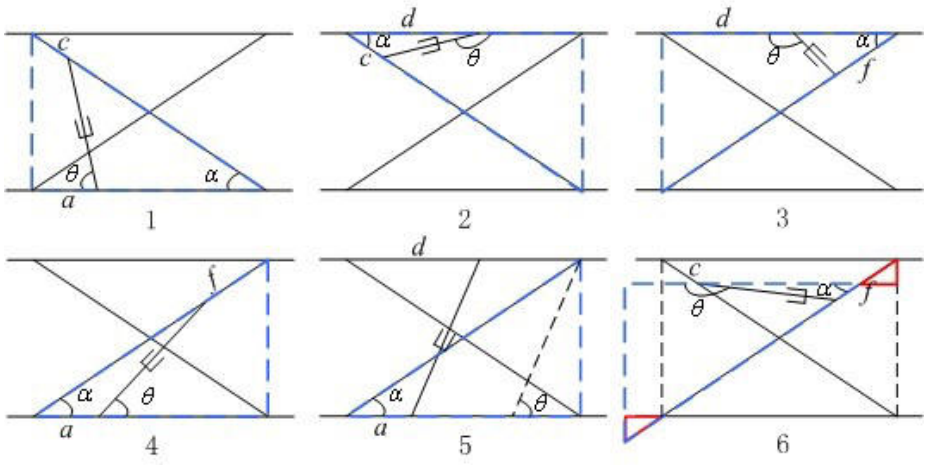

Fig. (1). Characteristic triangles of 6 different input configurations.

forces can be decomposed a sand. Since W is in the middle of the platform, the hypothesis is given. The first case is shown in Fig. (**4**).

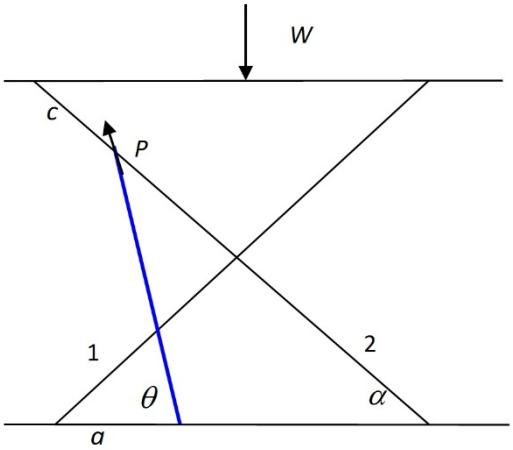

Fig. (2). Characteristic triangles of 6 different input configurations.

Table 1. Expressions of references between hydraulic force and load.

Case	1	2	3	4	5	6
M	*-c*	*c*	*f-2l*	*2l-f*	*0*	*c+f-2l*
N	*2l-c*	*c*	*f*	*2l-f*	*2l*	*f-c*

Table 2. Expressions of references of the six scissors.

Reference	1	2	3	4	5	6
c (mm)	200	200				200
f (mm)			200	200		400
a (mm)	300			548	200	
d (mm)		300	548		300	

$$Fy_1 = Fy_2 = -\frac{W}{2}$$

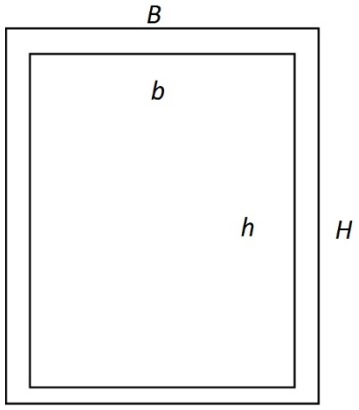

Fig. (3). Characteristic triangles of 6 different input configurations.

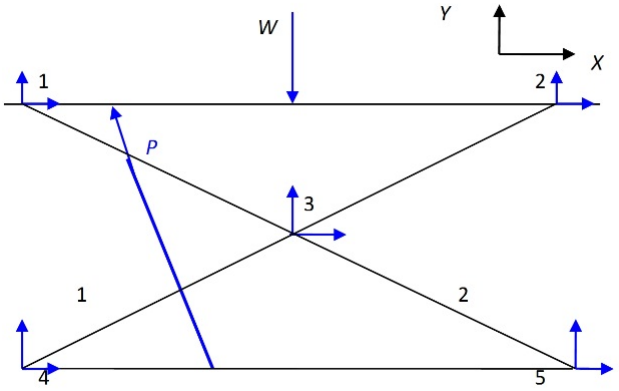

Fig. (4). Coordinate system and number of nodes in the scissor lifts.

The equilibrium of the force for the whole scissor:

$$-P\cos\theta + Fx_4 = 0 \tag{2}$$

$$-W + P\sin\theta + Fy_4 + Fy_5 = 0 \tag{3}$$

The equilibrium of the moment for the whole scissor:

$$-W\frac{L\cos\theta}{2} + Fy5L\cos\alpha + Pa\sin\theta = 0 \tag{4}$$

The equilibrium of the force for the scissor arm number 1:

$$Fx_3 = -Fx_4 \tag{5}$$

$$Fy_3 + Fy_4 - \frac{W}{2} = 0 \tag{6}$$

The equilibrium of the force for the scissor arm number 2:

$$-\frac{W}{2} + Fy_5 - Fy_3 + P\sin\theta = 0 \tag{7}$$

From (2) to (7) we can calculate the internal forces of nodes represented by W and P (See Table **3**).

Table 3. Expressions of internal forces for the first case.

Internal Forces of Nodes	*Fx*	*Fy*
1	0	$-\frac{W}{2}$
2	0	$-\frac{W}{2}$
3	$P\sin\theta$	$P\sin\theta - P\frac{a\sin\theta}{L\cos\theta}$
4	$P\sin\theta$	$\frac{W}{2} - P\sin\theta + P\frac{a\sin\theta}{L\cos\theta}$
5	0	$\frac{W}{2} - P\sin\theta$

4. STABILITY ANALYSIS OF SCISSOR ARM BY ENERGY METHOD

The total potential energy of an object is equal to the puissance of all forces from the stress state position to unstressed position. Since both the external force and internal force contributed to the puissance, the total potential energy expression is

$$\Pi = U + V \tag{8}$$

where U is internal potential energy V is outer energy. For an elastic body, U equals to outer puissance, therefore $\Pi = -U$

For a scissor arm, when the derivative of potential energy to the axial force equals 0, the arm is in equilibrium. When the second derivative of potential energy to the axial force is bigger than 0, the arm is in stable equilibrium. In this case the axial load is the critical load.

The first derivative of internal energy is:

$$dU = \frac{F^2 dx}{2EA} + \frac{M^2 dx}{2EI} \tag{9}$$

where F is the axial force, M is the moment of the arm.

Suppose the scissor arm can be divided into two parts of length l, the integration of internal energy is:

$$U = \int_0^l \left(\frac{F^2 dx}{2EA} + \frac{M_1^2 dx}{2EI}\right) + \int_l^{2l} \left(\frac{F^2 dx}{2EA} + \frac{M_2^2 dx}{2EI}\right) \tag{10}$$

where andare moments on the two parts of the arm.

The critical force F can be calculated by the derivation of U to F. When the derivation equals 0, the relevant force equals critical load.

Take the first case as an example. In order to analyze the stability of scissor arm, a simplification of boundary condition is given in Fig. (**5**).

Analyze the scissor arm number 1

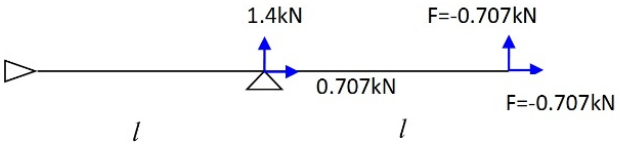

Fig. (5). Boundary condition of the scissor arm number 1 of first case.

Define V as the deflection of the scissor arm and we can get:

$$M_2 = F(V_{\max} + V_2 + l - x) \tag{11}$$

$$M_1 = F(V_{\max} + V_1) + Fl \tag{12}$$

When there are vertical and axial load on the arm, it is difficult to calculate the deflection. A simplification is made to help solve the problem: the deflection of scissor arm is made by axial load. Then we get the results:

$$V_1 = \frac{Fx(l^2 - x^2)}{6EI} \tag{13}$$

$$V_2 = \frac{Fx^3}{6EI} - \frac{Flx^2}{2EI} - \frac{Fl^2 x}{3EI} \tag{14}$$

$$V_{\max} = -\frac{2Fl^3}{3EI} \tag{15}$$

When we can calculate the critical load. The result is calculated in Matlab and we can get F_{cr} =21078 N. As for the arm number 2 as shown in Fig. (**6**), there is a hydraulic force at $x=c$, the axial force

$$F_2 = \left(\frac{W}{2} - P\frac{a\sin\theta}{l\cos\alpha}\right)\sin\alpha = 140\text{kN}$$

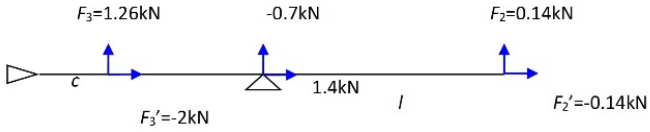

Fig. (6). Boundary condition of the scissor arm number 2 of first case.

Suppose there are vertical and axial load on the arm, for right arm, the deflection is

$$v = \frac{F_2 x(l^2 - x^2)}{6EI}$$

For left arm, we can divide it into two parts:

$$-\frac{F_3(l-c)x(x^2 - l^2 + (l-c)^2)}{6lEI} \qquad 0 \le x \le c$$

$$-\frac{F_3(l-x)c(x^2-l^2+(l-c)^2)}{6lEI} \qquad c \le x \le l \tag{16}$$

Now the scissor arm is composed of 3 parts

For the first part, 0<*x*<*c*: the deflection

$$V_1 = \frac{F_2 x(l^2-x^2)}{6EI} - \frac{F_3(l-c)x(x^2-l^2+(l-c)^2)}{6lEI} \tag{17}$$

The moment of this part:

$$M_1 = F_2 l + F(V_{\max}+V_1) + F_3(c-x) + F_3'(V_c - x) \tag{18}$$

The deflection at *x*=*c* is

$$V_c = \frac{F_2 c(l^2-c^2)}{6EI} - \frac{F_3(l-c)c(c^2-l^2+(l-c)^2)}{6lEI} \tag{19}$$

At the second part*c*<*x*<*l*, the deflection of this part is

$$V_2 = \frac{Fx(l^2-x^2)}{6EI} - \frac{F_3(l-x)c(x^2-l^2+(l-c)^2)}{6lEI} \tag{20}$$

The moment of this part is

$$M_2 = FL + F(V_{\max} - V_2) \tag{21}$$

The third part is the right arm:

$$V_3 = -\frac{Fx^3}{6EI} + \frac{FLx^2}{2EI} + (\frac{Fl^2}{3EI} + \frac{F_3(c^3-cl^2)}{6lEI})x \tag{22}$$

$$V_{\max} = \frac{2Fl^3}{3EI} + \frac{F_3}{6EI}(c^3-cl^2) \tag{23}$$

The moment of this part is

$$M_3 = F(V_{\max} - V_3 + l - x) \tag{24}$$

Integrate the internal energy *U* on the three parts of the scissor arm:

$$U = \int_0^c (\frac{F^2 dx}{2EA} + \frac{F_3'^2 dx}{2EA} + \frac{M_1^2 dx}{2EI}) + \int_c^l (\frac{F^2 dx}{2EA} + \frac{M_2^2 dx}{2EI}) + \int_0^l (\frac{F^2 dx}{2EA} + \frac{M_3^2 dx}{2EI}) \tag{25}$$

When the critical load is calculated, we have

$$\frac{dU}{dF} = 0 \quad , \quad \frac{d^2U}{dF^2} > 0$$

The critical load of the scissor arm number 2 of the first case equals to =21030 N.

$$F_{cr} = (\frac{W}{2} - P\frac{a\sin\theta}{l\cos\alpha})\sin\alpha$$
$$= W(\frac{1}{2} - \frac{2l}{(2l-c)\sin\theta + c\cos\theta\tan\alpha}\frac{a\sin\theta}{l\cos\alpha})\sin\alpha$$

=21030 N.

The critical axail force and the critical load of the 6 kinds of scissor lifts are calculated by using energy method. All the results are shown in the Table **4**. Since the fifth case is special, the scissor arm number 1 of the fifth case does not buckle or have a potential of losing stability under the boundary condition that is given, in this paper we only study the scissor arm number 2 of this case.

For each case of the scissor lifts, the final critical load equals the smaller critical load of its two scissor arms.

For each case of the scissor lifts, the final critical load equals the smaller critical load of its two scissor arms.

5. FEM MODELING ANALYSIS OF THE SCISSOR ARM

Finite element method is an efficient and approximating calculation method. It is also a method of numerical solution of solving field problem. The principle is dividing the continuous solution domain into a finite number of discrete units, find an approximate solution with the approximate function within each cell hypothesis, Then all the cells are combined to form a corresponding numerical model according to standard methods. In this paper MSC.Patran and MSC.Nastran are used to analyse the static stability of the scissor lift, the critical load of different cases are analysed in Nastran by using buckling analyse.

Take the first case as an example, the main steps of modeling in Patran are as follows:

1. Building the geometry model: build a curve, with its length 1200 mm, from the point (0, 0, 0) to the point (1200, 0, 0).

Table 4. Critical axial force and critical load of the scissor lift.

Case	1	2	3	4	5	6
expression $F_{cr,2}$	$\frac{W}{2}\sin\alpha$	$\frac{W-P\sin\theta}{2}\cos\alpha$	$\frac{W-P\sin\theta}{2}\cos\alpha$	$\frac{W}{2}\sin\alpha$		$\frac{W}{2}\sin\alpha$
expression $F_{cr,1}$	$\sin\alpha(\frac{1}{2}-P\frac{a\sin\theta}{l\cos\alpha})W$	$\frac{W}{2}\sin\alpha$	$\frac{W}{2}\sin\alpha$	$(P\frac{2(l-f)\sin(\theta-\alpha)}{2l\cos\alpha}-\frac{W}{2})\cos\alpha$	$(\frac{W}{2}-P\frac{a\sin\theta}{l\cos\alpha})\cos\alpha$	$\frac{W}{2}\cos\alpha$
$F_{cr,1}$	21078	21080	5240	16300		18700
$F_{cr,2}$	21030	20890	21080	21080	21080	20760
$W_{cr,1}$	59600	33460	52400	46110		62900
$W_{cr,2}$	297300	59090	59630	58560	112700	58730

2. Building meshes: build one dimension element to the curve and give 101 nodes.
3. Defining material: give aluminum to the scissor arm: Young's modulus equals 70 GPa, and poison ratio equals 0.3.
4. Defining property: give beam property (1D) to the arms.
5. Defining boundary conditions: boundary conditions correspond to the model's hypotheses
6. Defining load: the load correspond to the model's hypotheses, add a force of <-707, -707, 0> on the node of right edge.
7. Analyze: choose buckling analysis and obtain the buckling factor of first degree.
8. Access results: Access result of Nastran and get the buckling factor in patran.

Take the two scissor arms of the second case of scissor lift as the examples that modeled as type in Fig. (**7**), the buckling results are shown in Figs. (**8**, **9**).

The same analysis and the corresponding results of single scissor arm buckling critical load factor can be obtained through the six kinds of scissor lifts each. All the buckling factors and critical loads of the six kinds of scissor lifts are shown in Table **5**. For each case the smaller critical load of the two scissor arms is the critical load of the scissor lift.

Similarly to the results of the energy method, the scissor arm number 1 of the fifth case doesn't have a stability problem in the hypothesis of boundary condition given in the paper. Only the stability of scissor arm number 2 of fifth case is considered. Take the results of energy method and modeling method of the six cases of scissor lifts and make a comparison. The result is shown in Table **6**.

6. STATIC STABILITY ANALYSIS OF SCISSOR LIFT MODEL

The scissor lift model studied in this factor includes two scissor arms and a hydraulic actuator, the actuator is a cylinder model with the material of steel. Static stability analysis of the model includes scissor arm instability and hydraulic cylinder instability.

The property of the hydraulic actuator is one dimension element with Young's Modulus equals 200 Gpa and Poisson ratio equals 0.3.

When making the model of scissor lift, we select the lifting angle equals 15 degrees, 30 degrees and 45 degrees. Take the first case with lifting angle equals 45 degree as an example, the model is shown in Fig. (**10**).

For any kind of scissor lift, the minimum critical load values in the three cases is the critical load of the case. The critical buckling load factor and the modeling results obtained are shown in Table **7**.

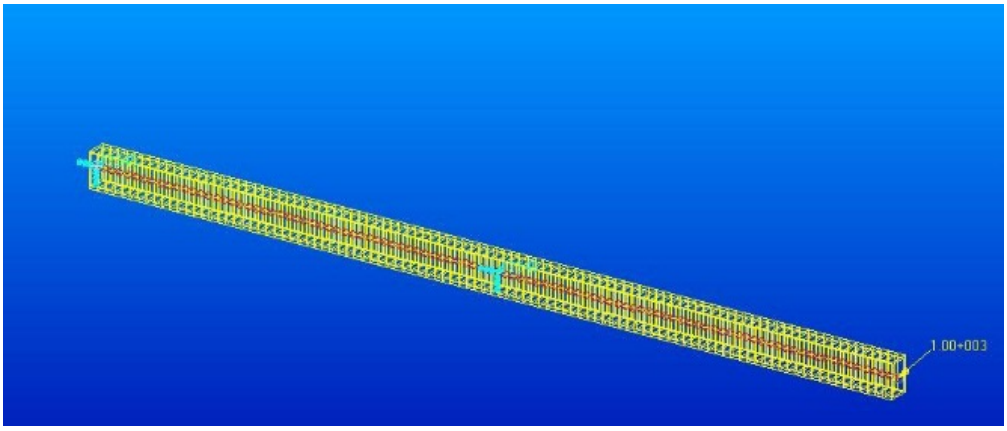

Fig. (7). The modeling of scissor arm in Patran.

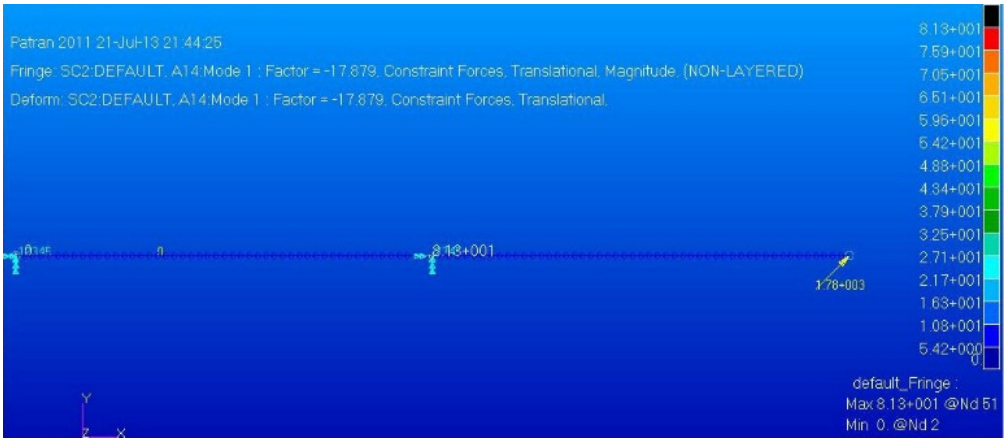

Fig. (8). Buckling results of the scissor arm number 1 of second case.

Fig. (9). Buckling results of the scissor arm number 2 of second case.

Table 5. Buckling factors and critical load of six cases of scissor lifts.

Case	1	2	3	4	5	6
W_energy (N)	59600	33460	52400	46110	112700	62900
W_modeling (N)	63730	35760	52800	46930	120500	64190
Difference (%)	6.5	6.4	0.76	1.7	6.5	2.0

Table 6. Comparison of energy method and modeling method of scissor arms' static stability.

Case	1	2	3	4	5	6
Factor1	31.86	-17.879	-26.413	-23.462		32.093
Factor2	160.91	31.86	31.863	-31.228	60.23	31.863
$F_{cr,1}$ (N)	22530	22530	5280	16590		22690
$F_{cr,2}$ (N)	22530	22530	22530	22480	22530	22530
$W_{cr,1}$ (N)	63730	35760	52800	46930		64190
$W_{cr,1}$ (N)	318670	63730	63730	62460	120500	63730

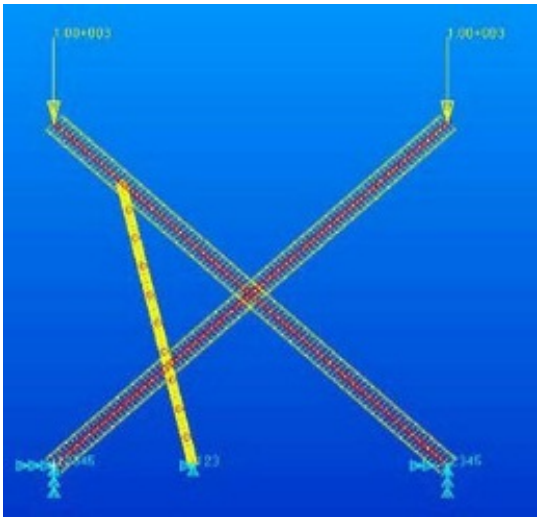

Fig. (10). Model of the first case of scissor lift.

After modeling and calculating six kinds of scissor lifts' critical load, the order of static stability of six cases from good to bad is: 5, 4, 1, 6, 2, 3.

CONCLUSION

This paper studies the static stability of six kinds of scissor lifts with one input force of hydraulic actuator, and the input is on the lines of the nodes of the scissor lifts. The static stability of six kinds of scissor lifts are compared.

For the stability analysis of single scissor arm, the results of two methods are basically consistent, which verified the accuracy of the single scissor arm critical loads. When using the finite element model to analyze the stability, the method Eigen value buckling analysis is used. The results of modeling and simulation is slightly larger than the energy analysis results, because the Eigen value buckling analysis result is considered as the upper limit of the critical load.

Table 7. The buckling factor and critical load of scissor lift models.

Case	1	2	3	4	5	6
Factor_15	12.56	1.97	1.43	13.59	35.755	11.88
W_15(N)	25120	3940	2860	27180	71510	23760
Factor_30	11.25	2.65	3.07	11.64	67.803	10.03
W_30(N)	22500	5300	6140	23280	135606	20060
Factor_45	9.89	3.22	5.2	10.01	87.939	8.70
W_45(N)	19780	6440	10400	20020	175878	17400
Critical load (N)	19780	3940	2860	20020	71510	17400

The stability results of single scissor arm and the scissor lift are compared. The results obtained from single scissor arm are better than the overall scissor lift model, which is due to its stronger boundary conditions. The results of the overall model are closer to the actual situation. By analyzing single arm models it is easier to compare theoretical solutions and modeling solutions, thus the study of stability of single scissor arm is meaningful.

CONFLICT OF INTEREST

The authors confirm that this article content has no conflict of interest.

ACKNOWLEDGEMENTS

This work is supported by National Natural Science Foundation of China and Civil Aviation Administration of China jointly funded project (Grant # U1233106), the Fundamental Research Funds for the Central Universities funded project (Grant # ZXH2012H007) and the university scientific research project of Civil Aviation University of China (Grant # 2012KYE05). Corresponding author is grateful to all who provided helps for this research.

REFERENCES

[1] E.L. Newlin, Waynesboro, *Work Platform Lift Machine with Scissor Lift Mechanism Employing Telescopable Electro-Mechanism Lift Actuation Arrangement*, US Patent US6044927A, 2000.

[2] T. Liu, and J. Sun, "Simulative calculation and optimal design of scissor lifting mechanism," In: *Chinese Control and Decision Conference*, Guilin, 2009, pp. 2079-2082.

[3] H. Tian, and Z. Zhang, "Design and simulation based on pro/E for A hydraulic lift platform in scissors type," *Journal of SciVerse ScienceDirect*, vol.16, pp. 772-781, 2011.

[4] A. Yenal, and G. C. Sobek, "Werner A novel adaptive spatial scissor-hinge structural mechanism for convertible roofs", *Journal of Engineering Structures*, vol. 33, no. 4, pp. 1365-1376, 2011.

[5] K. Guo, C. Pan, and X. Zhang, "A method of establishing and analyzing universal kinematics model based on plane scissor-like element, " *Journal of Machine Design and Research*, vol. 26, no. 6, pp. 27-30, 2010.

[6] I. Raskin, *Stiffness and Stability of Deployable Pantographic Columns*, PhD Thesis, University of Waterloo, Waterloo, Ontario, 1998.

Received: February 17, 2014 Revised: March 21, 2015 Accepted: June 9, 2015